Pharmaceutical Research, Vol. 7, No. 3, 1990

Research Article

Transport Mechanisms in Iontophoresis. III. An Experimental Study of the Contributions of Electroosmotic Flow and Permeability Change in Transport of Low and High Molecular Weight Solutes

Michael J. Pikal[1,2] and Saroj Shah[1]

Received March 20, 1989; accepted August 1, 1989

The objective of this research was to provide *in vitro* transport data designed to clarify the relative importance of permeability increase and electroosmotic flow in flux enhancement via iontophoresis. Iontophoretic fluxes were measured with both anode and cathode donor cells, and passive fluxes were measured both before iontophoresis (Passive 1) and after iontophoresis (Passive 2). Data were generated for three uncharged low molecular weight solutes (glycine, glucose, and tyrosine) and two high molecular weight anionic species (carboxy inulin and bovine serum albumin). Flux enhancement is greater for anodic delivery than for cathodic delivery, even for the negatively charged molecules, and anodic flux of glucose decreases as the concentration of NaCl increases. Both observations are consistent with a mass transfer mechanism strongly dependent on electroosmotic flow. Steady-state anodic flux at 0.32 mA/cm^2, expressed as equivalent donor solution flux (in μl/hr cm^2), ranged from 6.1 for glycine to about 2 for the large anions. As expected, iontophoretic flux is higher at 3.2 mA/cm^2 than at 0.32 mA/cm^2, and passive flux measured after iontophoresis is about a factor of 10 greater than the corresponding flux measured before the skin was exposed to electric current. There are two mechanisms for flux enhancement relative to passive flux on "fresh" hairless mouse skin: (1) the effect of the voltage in increasing mass transfer over the passive diffusion level, the effect of electroosmotic flow dominating this contribution in the systems studied in this report; and (2) the effect of prior current flow in increasing the "intrinsic permeability" of the skin. Both effects are significant. Based on theoretical results given elsewhere, theoretical values for flux were calculated and compared with the experimental data. While agreement between theory and experiment was only qualitative in several cases, most of the data are predicted quantitatively by the theory.

KEY WORDS: transdermal; iontophoresis; electroosmosis; mechanisms of iontophoresis; permeability change; molecular weight dependence.

INTRODUCTION

Volume flow via electroosmosis is a probable mechanism for enhanced transport of both charged and neutral species via iontophoresis (1–5). However, the observed decrease in electrical resistance of hairless mouse skin after passage of DC current (2,6) and the apparent increased passive transport of neutral species following a period of iontophoresis (5) suggest that permeability is also increased by iontophoresis. The objective of this paper is to provide *in vitro* transport data which are designed to clarify the relative importance of permeability increase and volume flow. The experimental protocol includes measurement of solute fluxes during anodic and cathodic iontophoresis as well as passive fluxes before and after iontophoresis. Data are generated for three uncharged low molecular weight solutes (glycine, glucose, and tyrosine) and two high molecular weight anionic species (carboxy inulin and bovine serum albumin). Comparison of the experimental fluxes and a comparison of experimental fluxes with theoretical results (1), are used in an attempt to clarify the mechanisms for enhanced transport via iontophoresis.

EXPERIMENTAL

Materials

Radiotracers, all obtained from Amersham, were as follows: D-[1-^{14}C]glucose, [1-^{14}C]glycine, L-[carboxyl-^{14}C]tyrosine, inulin-[^{14}C]carboxylic acid, and [^{14}C]methylated bovine serum albumin. Buffers, sodium chloride, and nonradioactive analogue of the radiotracers were either reagent grade or obtained from Sigma [inulin (from chicory root), bovine serum albumin (crystallized and lyophilized), L-tyrosine]. The water was water for injection (Eli Lilly & Co.). All materials were used without further

[1] Lilly Research Laboratories, Eli Lilly and Co., Indianapolis, Indiana 46285.

[2] To whom correspondence should be addressed.

0724-8741/90/0300-0222$06.00/0

purification. The hairless mouse skin was full thickness dorsal skin obtained as previously described (2). The skin sample was equilibrated prior to use by soaking in the solution of interest overnight at 5°C (2).

Apparatus and Procedures

Volume flow and electrical resistance measurements were made using the same apparatus and procedures described in the second paper of this series (2).

Valia-Chien permeation cells (Crown Glass) with Ag/AgCl electrodes placed in the solutions through the filling and sampling ports were used for the iontophoresis studies. The electrodes fitted loosely and a small air head space was left above the solution level in each half-cell to ensure that volume flow would not induce hydrostatic pressure differences. The electrodes were similar to the "probe" electrodes described earlier (2). Constant current was delivered by a power supply (General Resistance Model E-35), and the actual current passed was checked by a digital ampmeter (Fluke, Model 8020B). Except for the radioactive tracer in the donor side, the solutions on the donor and acceptor sides of the cell were identical. Due to the porous nature of the electrodes, it was necessary to soak the electrodes for at least 24 hr following an experiment to avoid problems of residual radioactivity leaching into the solution in the next experiment. All experiments were carried out at 37°C.

The procedure used for studies at 0.2 mA involved using skin from one mouse to supply the membranes for two permeation cells. One cell was equipped with electrodes and was used to study transport by iontophoresis at 0.2 mA (0.32 mA/cm^2). The other cell was used to follow passive transport. Thus, the skin sample used to study passive transport was never exposed to current flow. For both cells, solution samples were taken at 2, 4, 6, 8, and 24 hr.

An alternate procedure was used for a direct comparison of passive and iontophoretic flux. Again, skin from one mouse was used for two permeation cells where the anode was always on the stratum corneum side of the skin. Each cell was subjected to the sequence (a) passive (no current) for 3 hr, (b) iontophoresis at 2 mA (3.2 mA/cm^2) for 3 hr, (c) passive for 18 hr. In one cell the anode was the donor side during iontophoresis, while in the other cell the cathode was the donor. In preliminary experiments with glucose, a number of experiments were run where a 3-hr passive period was placed between the iontophoretic period and the 18-hr passive period. Within experimental error, the fluxes for both postiontophoretic passive periods were identical.

It should be noted that while the pH remains constant during current flow, the concentration of NaCl is decreased at the anode and increased at the cathode. Thus, while the experiment begins with the same solution (except for radiotracer) on both sides of the membrane, a concentration difference develops with time. At the end of a 24-hr period of 0.2 mA, the concentration difference is $\approx$0.038 *M*, while at the end of 3 hr at 2 mA, the corresponding difference is $\approx$0.047 *M*. This concentration difference produces an osmotic pressure difference which may, in principle, affect transport behavior.

In an effort to estimate the degree of enzymatic degradation of bovine serum albumin (BSA) during an iontophoresis experiment, two replicate "fraction collection" experiments were run. In one permeation cell, radiotracer was placed on the stratum corneum side and cathodic iontophoresis was carried out for 24 hr at 0.2 mA. In the other cell, radiotracer was placed on both stratum corneum and dermis sides, and the system was allowed to "react" for 24 hr with no current. Samples from both cells were taken initially and after 24 hr. All samples were separated into five molecular weight fractions by size-exclusion HPLC, and each fraction was counted for total radioactivity. A DuPont GF250 column was used at ambient temperature with a mobile phase consisting of 0.025 *M* NH_4HCO_3 adjusted to pH 7 with H_3PO_4. At a flow of 1 ml/min, the retention time of monomeric BSA was 7.1 min. An enzymatic digest (*S. aureus* protease) of BSA gave a mixture with peaks between 7.1 and 12 min. Glycine was detected at 12.6 min. The retention time intervals, in minutes, corresponding to the five fractions was (1) 6.0–7.0, (2) 7.0–7.5, (3) 7.5–8.5, (4) 8.5–10.5, and (5) 10.5–13.0. The molecular weight range corresponding to each fraction was estimated by assuming that the logarithm of molecular weight is linear in retention time and "calibrating" and monomeric BSA (69 kD), ovalbumin (43 kD), and human growth hormone (22 kD). While extrapolation of this calibration curve much lower than 15 kD (fractions 4 and 5) is somewhat uncertain, we note that the calculated molecular weight for glycine is in error by only 22%.

RESULTS

Some relevant physical properties of the compounds studied are summarized in Table I. Note that while both glycine and tyrosine are partially in the anionic form at the pH studied, each of these compounds is mostly in the zwitterion or neutral form. Carboxy inulin is assumed to have a "typical" carboxyl pK_a (4.8) and therefore should be essentially anionic at pH 8.5. Bovine serum albumin (BSA) has an isoelectric point of 4.7 (8) and therefore is anionic at pH 8.5. However, in spite of a high formal negative charge (indicated by the primary structure), the effective charge calculated from the measured electrophoretic mobility (8) is quite small, presumably reflecting extensive counterion condensation typical of a polyelectrolyte (15). The Stokes radius is the effective radius of a molecule for motion through a solvent, as calculated from the tracer diffusion data in aqueous systems according to the Stokes–Einstein equation (1).

Volume flow and electrical resistance measurements were made at 1 mA/cm^2 for hairless mouse skin in contact with a solution of the following composition: 0.05 *M* glucose/0.1 *M* NaCl/0.01 *M* Tris buffer (pH 8.5). The area-normalized electrical resistance is 704 Ω cm^2, compared with 710 Ω cm^2 for 0.1 *M* NaCl (2). The volume flow, J_v, in units of μl/hr cm^2, is 10.0 $\pm$ 0.8 with the stratum corneum facing the anode and 14.0 $\pm$ 1.1 with the dermis facing the anode. The volume flow appears to be slightly higher for the glucose/Tris-containing solution than for pure 0.1 *M* NaCl (2). It is clear, however, that volume flow and electrical resistance of hairless mouse skin are not greatly altered by either the Tris buffer system or glucose. Therefore, we assume that the electroosmotic flow data generated earlier (2) apply at least semiquantitatively to the iontophoresis studies described in this report.

Table I. Selected Properties of Compounds Studied

Compound	MW	pH	% Neutral[a]	% Anion	Anion Charge[b]	Stokes Radius (Å)[c]
Glycine	75	8.5	95	5	−1	2.3
Glucose	180	8.5	100	0	—	3.6
Tyrosine	181	8.5	80	20	−1	9.4
Carboxy inulin	5,200	8.5	0	100	−1	11.0
		3.9	89	11	−1	11.0
BSA	69,000	8.5	0	100	−0.35	35.0

[a] Calculated from estimated (carboxy inulin) or tabulated pK_a data (7) and isoelectric point for BSA (8).
[b] Determined by chemical structure or, for BSA, calculated from the diffusion constant and the electrophoretic mobility (8) using the Nernst–Einstein equation (9).
[c] Calculated from the tracer diffusion coefficient data using the Stokes–Einstein equation. Diffusion data were taken from the literature: glycine (10), glucose (11), tyrosine (12), carboxy inulin (13), and BSA (14).

Figures 1 and 2 summarize comparative iontophoretic (0.32 mA/cm^2) and passive flux data for small "mostly neutral" molecules (Fig. 1) and anionic high molecular weight molecules (Fig. 2), all delivered from the anode compartment of the transport cell. Fluxes are expressed as volume flux of donor solution, J_{vs}, in μl/hr cm^2. The relationship between molar flux of species 1, J_1, and solution flux is $J_1 = J_{vs}\, c_1^o$, where c_1^o is the concentration of species 1 in the donor solution in mol/cm^3. The passive fluxes, which average roughly 0.1 μl/hr cm^2, are at the limit of detectability and are therefore only semiquantitative at best. Passive fluxes were measured on skin samples not previously exposed to electrical current. Each data point is the mean of three to six replicate experiments, with the vertical bar representing the standard error of the mean. Results for the large molecules (Fig. 2) were much less reproducible, evidently reflecting, for the most part, variation between samples of skin. The large uncertainties in Fig. 2 obscure any potential time dependence for transport of carboxy inulin or BSA. The mean values of solution flux are 2.3 ± 0.4 (carboxy inulin) and 2.6 ± 0.3 (BSA). It should be emphasized that all transport data are based on transport of total radioactivty. One might question this assumption for a large protein.

Since one might expect some enzymatic degradation of a protein during transport through skin, the distribution of radioactivity among five molecular weight fractions was examined for BSA solutions which had been exposed to hairless mouse skin (Fig. 3). The experiment is based on determining the relative radioactivity in selected molecular weight fractions separated by size exclusion HPLC. The filled bars represent the initial sample, and the open bars represent the distribution of radioactivity in the material transported. The various degrees of shading represent distributions of radioactivity in BSA solutions which had been exposed to stratum corneum or dermis under conditions of no current flow or cathodic iontophoresis at 0.32 mA/cm^2. These "shaded" distributions are not significantly different from the initial distribution, but the distribution of transported radioactivity (open bars) is significantly altered. The implication of these observations is discussed later.

Anodic and cathodic iontophoresis at 3.2 mA/cm^2 are compared with passive transport in Fig. 4. Passive transport measured prior to exposure of the skin to electrical current is denoted "Passive 1," while passive transport measured after the three hour iontophoresis period is referred to as "Passive 2." Note that while the Passive 2 experiments were conducted under an osmotic pressure difference (see Experimental), the resulting hydrodynamic flow is negligible (see Theoretical). The lighter shaded bars refer to an anodic donor during iontophoresis while the darker shading represents a cathodic donor. Each bar represents the mean of replicate measurements: 7 replicates for glucose, 12 for carboxy inulin at pH 8.5, and 3 for carboxy inulin at pH 3.9. The error bar represents the standard error of the mean. The error bar for cathodic delivery of carboxy inulin at pH 3.9 is unusually large due to nonreproducibility and the low number of replicates. However, it should be noted that in each of the three replicate experiments, the cathodic flux was significantly greater than the anodic flux. The passive flux measured before current was applied, denoted Passive 1, averaged 0.2 μl/hr cm^2, the same magnitude as measured in the experiments summarized by Figs. 1 and 2. Again, flux of this magnitude is at the limit of detectability and is not quantitative. With the possible exception of the data in Fig. 4C, passive transport measured after current flow of 3.2 mA/cm^2 (Passive 2) is roughly one order of magnitude larger than passive transport measured before current flow (Passive 1). The exception noted for carboxy inulin at low pH may not be real, as the Passive 2 data given in Fig. 4C represent the mean of only two replicates that were in poor agreement.

The effect of NaCl concentration on iontophoretic and passive flux of glucose solution is shown in Fig. 5. Data shown are the means of replicate experiments: four replicates at 0.5 *M*, seven at 0.1 *M*, and five replicates at 0.5 *M* NaCl. Error bars represent the standard error of the mean. The iontophoretic flux, denoted "IONTO(2 mA)," refers to flux measured from an anodic donor with 2-mA current (3.2 mA/cm^2). Cathodic flux (not shown) is not significantly different from the corresponding Passive 2 flux, the mean ratio of cathodic flux to Passive 2 flux being 1.04 ± 0.07. Passive 2 flux is independent of whether the donor was anodic or cathodic during iontophoresis , and the data given in Fig. 5 are the means of the two polarity cases. (The mean ratio of Passive 2 fluxes, anode donor:cathode donor, is 1.08 ± 0.25 for the glucose experiments.)

THEORETICAL

The theoretical analysis presented earlier (1) considered flux enhancement in a system where both sides of the mem-

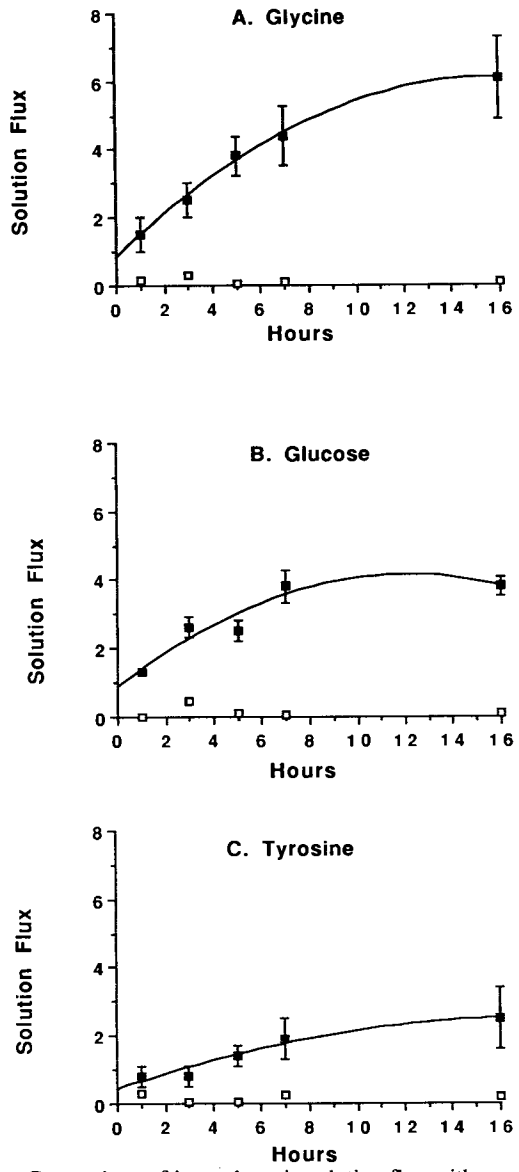

Fig. 1. Comparison of iontophoretic solution flux with passive solution flux through hairless mouse skin for small molecules at 37°C. Solid symbols are for iontophoresis at 0.32 mA/cm^2 with the donor side containing the anode, while open symbols are for passive (diffusional) transport. The stratum corneum faces the donor. All solutions are 0.1 *M* NaCl and 0.01 *M* Tris buffer at pH 8.5. Nonradioactive glycine and glucose are 0.05 *M*, and tyrosine is 0.002 *M*. Solution flux is equivalent transport of donor solution, J_{vs}, in units of $\mu l\ hr^{-1}\ cm^{-2}$.

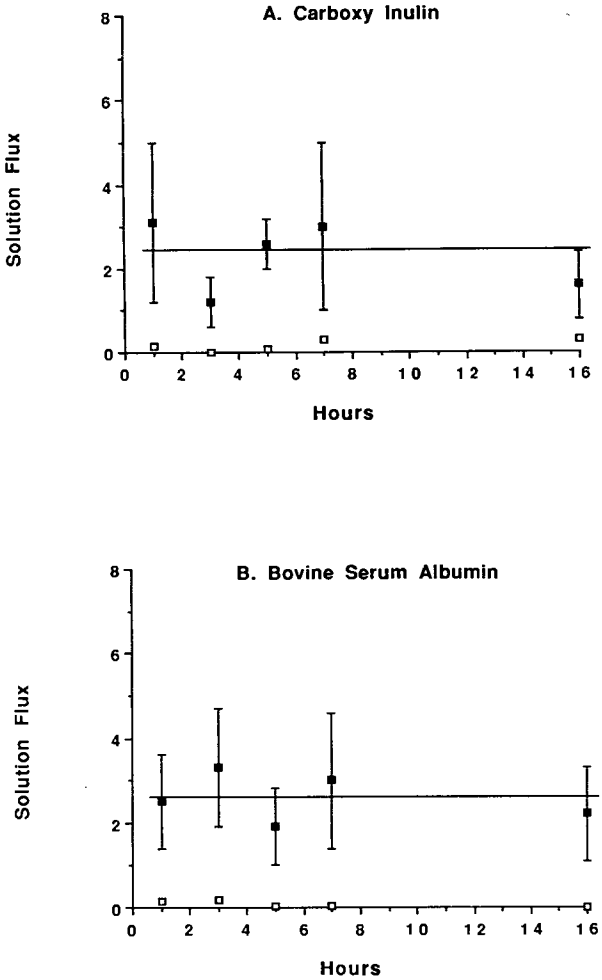

Fig. 2. Comparison of anodic iontophoretic solution flux with passive solution flux through hairless mouse skin for large molecules at 37°C. Solid symbols are for iontophoresis at 0.32 mA/cm^2 with the donor side containing the anode, while open symbols are for passive (diffusional) transport. The stratum corneum faces the donor. All solutions are 0.1 *M* NaCl and 0.01 *M* Tris buffer at pH 8.5. The carboxy inulin solution contains 0.9 mg/ml nonradioactive inulin, while the bovine serum albumin solution contains 0.2 mg/ml nonradioactive bovine serum albumin. Solution flux is equivalent transport of donor solution, J_{vs}, in units of $\mu l/hr^{-1}\ cm^{-2}$.

brane are in contact with solutions of the same composition, except for tracer species. In some experiments, including those described in this report, significant concentration changes occur during iontophoresis, resulting in an osmotic pressure difference across the membrane, which, in turn, could produce significant volume flow. The concentration is decreased on the anode side and increased on the cathode side, which gives a higher osmotic pressure on the anode side, thereby inducing hydrodynamic flow from anode to cathode. The contribution of this effect to flux enhancement may be developed using the same model described previously (1). Briefly, the concentration difference between cathode side and anode side, Δc (mol/ml), produces an osmotic pressure difference between anode and cathode sides, $\Delta\pi$, where for an ideal 1-1 electrolyte, $\Delta\pi = 2RT\,\Delta c$. Here, R is the gas constant and T is the absolute temperature. This osmotic pressure difference produces volume flow through each type of membrane pore from anode to cathode according to Poiseuille's law and, for a negatively charged pore, adds to the volume flow produced by electroosmotic flow. The flux enhancement ratio is given by the same formal relationship developed earlier (1), which expressed in terms of J_{vs}, is

$$J_{vs}/J_{vs}^{D} = \Sigma A_i\,\alpha_i\,[1-\exp(-\alpha_i)]^{-1} \qquad (1)$$

where the summation is over all three pore types (positive,

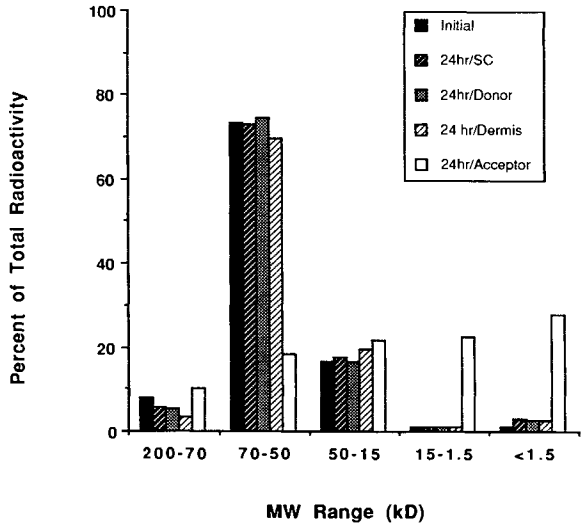

Fig. 3. Decomposition of bovine serum albumin during iontophoresis experiments with hairless mouse skin at 37°C: distribution of radioactivity in selected molecular weight ranges. Distributions: Initial = prior to exposure to skin sample; 24 hr/SC = 24 hr of exposure to stratum corneum without current flow; 24 hr/Dermis = 24 hr of exposure to dermis without current flow; 24 hr/Donor = donor side (stratum corneum) after 24 hr of cathodic iontophoresis at 0.32 mA/cm^2; 24 hr/Acceptor = acceptor side (transported radioactivity) after 24 hr of cathodic iontophoresis at 0.32 mA/cm^2. Mean equivalent solution flux, J_{vs}, based on total transported radioactivity is 1.2 ± 0.2 μl/hr cm^2. All solutions are 0.1 *M* NaCl and 0.01 *M* Tris buffer at pH 8.5 and contain 0.2 mg/ml nonradioactive bovine serum albumin.

neutral, and negative) and α_i is the flux enhancement parameter for each pore type *i*. The term, A_i, is the area fraction effective for transport in pore *i* (Eq. 32, Ref. 1). The A_i term not only includes the effect of different pore radii (positive pores, 6.75 Å; neutral pores, 13.5 Å; and negative pores, 27 Å), but also includes the effects of the distribution (partition) coefficient and reflection coefficient (1). The flux enhancement parameter, α_i, is specific to the pore type (charge and size) and is given by the sum of the previous result (Eq. 30, Ref. 1) and the osmotic pressure contribution, α_c,

$$\alpha_c = 1.5\ \pi \cdot 10^{-3}\ N_o\ a\ r_i^2\ \Delta C \qquad (2)$$

The symbols are as follows: ΔC (mol/L) = concentration difference between receiver and donor sides; N_o = Avogadro's number; a = Stokes radius of species 1; and r_i = pore radius of the membrane pores of type i. Note that in the "Passive 2" experiments where no voltage is applied, J_{vs} (anode)/J_{vs} (cathode) = exp(α_c). Using the "average" pore radius relevant for pure osmotic flow given from theory, 17 Å (1), the predicted anode:cathode flux ratio for Passive 2 experiments with glucose is 1.15, compared with the experimental value of 1.08 ± 0.25. The corresponding comparison for carboxy inulin is 1.5, compared to an experimental value of 2 ± 1. Thus, even for Passive 2 experiments, where the osmotic pressure effect is greatest, the effect is less than experimental error in the fluxes. Therefore, the osmotic pressure effect is ignored in the balance of this discussion.

Theoretical values of solution flux may be evaluated from Eqs. (1) and (2) provided that a theoretical estimate of

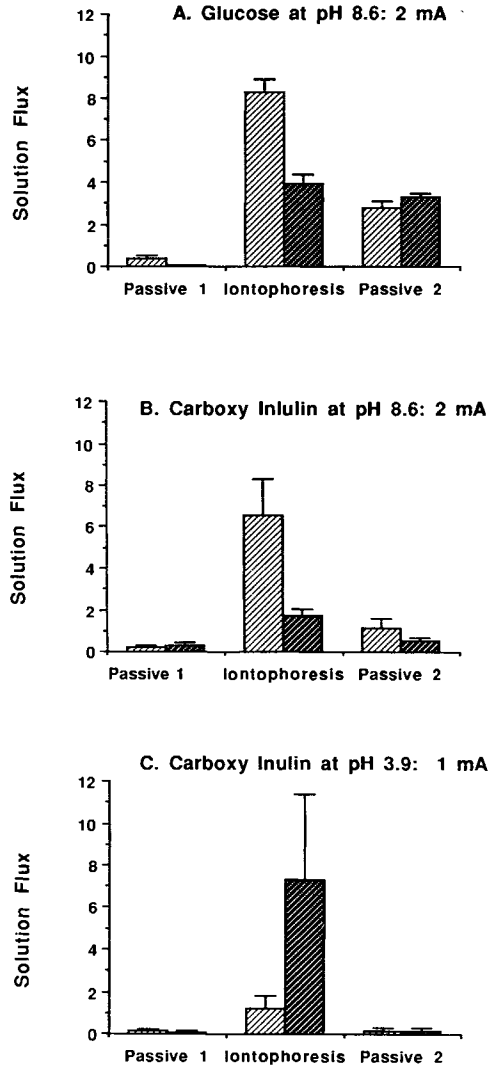

Fig. 4. Comparison of anodic and cathodic iontophoresis at 3.2 mA/cm^2 with passive transport preiontophoresis (Passive 1) and postiontophoresis (Passive 2) for hairless mouse skin at 37°C. Light shading refers to anodic donor during iontophoresis, while dark shading corresponds to a cathodic donor. The stratum corneum faces the anode. Solution fluxes, J_{vs}, in units of μl hr^{-1} cm^{-2}, are measured over time intervals of 3 hr (Passive 1), 3 hr (iontophoresis), and 18 hr (Passive 2). The glucose solution contains 0.05 *M* nonradioactive glucose, and the carboxy inulin solutions contain 0.9 mg/ml nonradioactive inulin. All solutions contain 0.1 *M* NaCl. Tris buffer (0.01 *M*) is used at pH 8.6, while citrate buffer (0.01 *M*) is used at pH 3.9.

passive solution flux, J_{vs}^D, is available. The theoretical model described previously (1) leads to the expression for J_{vs}^D, in units of μl/hr cm^2,

$$J_{vs}^D = 3.6 \cdot 10^6 (f/\eta_r L)\ (kT/6\pi\eta_o a)\ (\langle P \rangle) \qquad (3)$$

where f is the fraction of membrane area which is pore area, L is the pore length, η_r is the viscosity of the pore fluid relative to pure water at the reference temperature, taken as 25°C, η_o is the viscosity of pure water at the reference temperature, k is Boltzmann's constant, $\langle P \rangle$ is the mean value of the product, $K_1^i(1-\sigma_i)$, where K_1^i is the partition coefficient

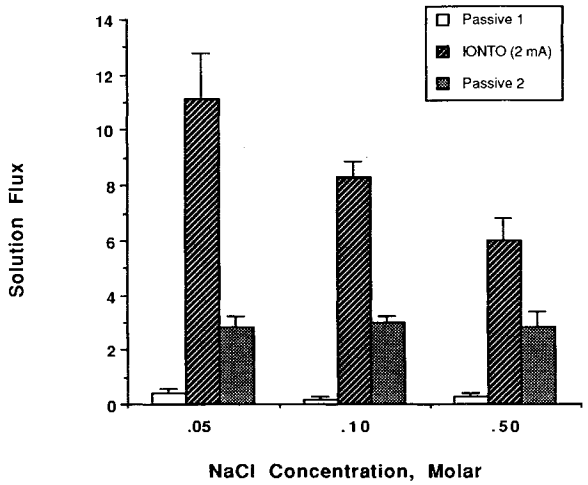

Fig. 5. The effect of NaCl concentration on iontophoretic delivery of glucose through hairless mouse skin at 37°C. The iontophoresis data shown (denoted "IONTO") refer to anodic delivery at 3.2 mA/cm^2 with the stratum corneum facing the anode. Solution fluxes, J_{vs}, in units of μl hr^{-1} cm^{-2}, are measured over time intervals of 3 hr (Passive 1), 3 hr (iontophoresis), and 18 hr (Passive 2). Corresponding cathodic fluxes (not shown) are not significantly different from the Passive 2 fluxes. All solutions contain 0.05 *M* nonradioactive glucose buffered to pH 8.6 with 0.01 *M* Tris buffer.

for species 1 in pore type *i*, and σ^i is the reflection coefficient for species 1 in pore type *i* (1). The partition coefficient may be calculated, but at best, the reflection coefficient can only be roughly estimated. The group of terms, $(f/\eta_r L)$, might be termed an "intrinsic" membrane permeability and may be estimated from the electrical resistance of the membrane, measured under "appropriate" conditions, and the conductivity of the electrolyte in contact with the membrane (1,2). As "appropriate" conditions, we use the following: Passive 1—resistance measured at zero current density (extrapolated) on skin not previously exposed to current, $(f/\eta_r L)$ = 0.010; Passive 2—resistance measured at zero current density (extrapolated) on skin previously exposed to current densities of 1–2 mA/cm^2 for at least 1 hr, $(f/\eta_r L)$ = 0.083; and iontophoresis —resistance measured at the relevant current density on skin previously exposed to current densities of 1–2 mA/cm^2 for at least 1 hr, $(f/\eta_r L)$ = 0.092 (0.32 mA/cm^2), $(f/\eta_r L)$ = 0.166 (3.2 mA/cm^2). We take $K_1{}^i$ = 1 for neutral species, and σ_i = 0 for all species. While the partition coefficient of a neutral species should be close to unity to be consistent with the pore model (1), the reflection coefficient for a large molecule (carboxy inulin, BSA) may be significantly larger than zero, particularly for the small positive pores. Therefore, some pores effective for transport of sodium and chloride ions (reflected in "$f/\eta_r L$") are too small to be effective in transport of the large molecule, and the flux for large molecules may be overestimated by this procedure. Finally, to evaluate α_i, an estimate of voltage drop $(-\Delta\Phi_v)$ across the hairless mouse skin is needed. From experimental resistance data (Fig. 4 and footnote 6 in Ref. 2), the mean voltage drop is estimated to be 0.24 V for the experiments at 0.32 mA/cm^2 and 1.35 V for the experiments at 3.2 mA/cm^2.

It should be emphasized that the above values for $f/\eta_r L$ and voltage drop are *estimates* which are based on interpolation and extrapolation of resistance data (2). Perhaps the most dubious extrapolation is the assumption that changes in the properties of skin brought on by prior passage of current in the range of 1–2 mA/cm^2 are representative of changes induced by current densities of 0.32 and 3.2 mA/cm^2. Fortunately, errors in resistance estimation will partly cancel in calculation of flux. For example, if the resistance estimate is too large, $f/\eta_r L$ will be too small, but the voltage estimate will be proportionately too large, leaving the calculated iontophoretic flux largely unchanged as long as α_i for the pore types dominating transport are significantly greater than unity.

DISCUSSION

While the molecular weight distribution of the radioactive BSA changes but little after contact with stratum corneum or dermis for 24 hr, the distribution of the transported BSA is significantly different from the initial sample (Fig. 3). Monomeric BSA (70–50 kD) has apparently been converted to lower molecular weight species (15–1.5 and <1.5 kD) during transport. One might also argue that the data (Fig. 3) suggest preferential transport of small species present in the initial sample as impurities. However, preferential transport alone cannot explain the observed distributions (Fig. 3) without requiring unrealistic J_{vs} values. Assuming no degradation during transport, J_{vs} (μl/hr cm^2) for each fraction is calculated from the distribution data as 2.0 (fraction 1), 0.27 (fraction 2), 1.6 (fraction 3), 36.3 (fraction 4), and 9.9 (fraction 5). It is difficult to believe that dimer (fraction 1) would be transported nearly an order of magnitude more efficiently than monomer (fraction 2). Also, the molecular weight (and Stokes radius) represented by fraction 4 is in the same range as carboxy inulin. Since only anionic species could be transported with any efficiency in cathodic delivery at neutral or alkaline pH (1), anionic carboxy inulin should be a reasonable model for cathodic transport of fraction 4. However, even at 3.2 mA/cm^2, cathodic flux of carboxy inulin is only 1.7 μl/hr cm^2, which is far less than the "measured" fraction 4 flux. While preferential transport of impurities may not be negligible, it appears that the major effect is degradation during transport. Therefore, we tentatively conclude that flux of total radioactivity is a good first approximation to flux of intact BSA through the barrier (stratum corneum) but significant degradation occurs *during transport,* presumably during transport through the viable epidermis or dermis. While extrapolation of this information to proteins in *in vivo* experiments is uncertain, it seems likely that although proteins may be transported via iontophoresis, significant degradation will occur. Note that the only degradation addressed in this report is change in molecular weight. Other decomposition pathways that affect activity may also be significant.

At least for small molecules at low current density, steady state is not reached until after ≈8 hr (Fig. 1). Similar observations have been made by Burnette and co-workers for mannitol in human skin (4) and a tripeptide in hairless mouse skin (3). A theoretical non-steady-state analysis of iontophoresis (ignoring the contribution of electroosmotic flow) suggests that the approach to steady state is much

faster under conditions of high flux enhancement parameter, α_i (16). If one assumes that the same qualitative result is valid when electroosmotic flow is significant, flux measured at higher current density should reach steady state more quickly. Thus, the fluxes measured at 3.2 mA/cm^2 (Figs. 4 and 5), which correspond to a time of 1.5 hr, would be much closer to steady state than the corresponding fluxes at 1.5 hr measured at 0.32 mA/cm^2 (Figs. 1 and 2).

Equivalent solution flux, J_{vs}, in units of μl/hr cm^2, is numerically identical to molar flux, J_1, in units of nmol/hr cm^2 when the donor solution is 1 m*M* in component 1. Thus, the results given by Burnette and Ongpipattanakul for steady-state molar flux of mannitol in human skin (4) are equivalent to $J_{vs} \approx 0.8$ μl/hr cm^2 at 0.23 mA/cm^2, which is about a factor of 5 less than the corresponding flux measured for glucose in HMS at 0.32 mA/cm^2. Since electroosmotic flow in human skin (17) is about a factor of 7 higher than in HMS (1,2), one would expect mannitol flux in human skin to be higher than glucose flux in HMS. We have no satisfactory interpretation for this apparent anomaly.

Using "Passive 1" flux as a baseline, iontophoresis results in significant flux enhancement (Figs. 1, 2, and 4). At pH 8.5 where the net charge in HMS remains negative during passage of high current (2), flux enhancement is greater for anodic delivery than for cathodic delivery, even for an anion (Fig. 4). Note also (Fig. 5) that anodic glucose flux decreases with increasing NaCl concentration in the same manner as does the electroosmotic flow (2). Both results are consistent with a mass transfer mechanism strongly dependent on electroosmotic flow, which drives transport from anode to cathode for a membrane of negative charge. At pH 3.9, electroosmotic flow from anode to cathode was observed to decrease sharply with time at high current density and occasionally to reverse in direction (2). Thus, at pH 3.9, one would expect cathodic flux of negatively charged carboxy inulin to be greater than the corresponding anodic flux, as observed. The unusually large error bars noted in Fig. 4C may be related to the erratic electroosmotic flow behavior of HMS at low pH and high current density (2). Consistent with previous observations (5), the passive flux measured after current flow through a skin sample (Passive 2) is much larger than the corresponding passive flux measured on "fresh" skin (Passive 1). The ratio of Passive 2 flux to Passive 1 flux for a given compound (about a factor of 10) is quantitatively consistent with the electrical resistance data (2), which are reflected in the "intrinsic permeability" data, $f/\eta_r L$ (see Theoretical). Thus, the "intrinsic permeability" of HMS increases significantly after (and presumably during) current flow, suggesting that Passive 2 flux is a better measure of the passive contribution during iontophoresis than is the Passive 1 flux. Indeed, the appropriate value of passive flux during iontophoresis at 3.2 mA/cm^2 is a factor of 2 greater than the Passive 2 flux due to reversible changes in electrical resistance during current flow; i.e., the value of $f/\eta_r L$ is taken as 0.166 for passive flux during iontophoresis at 3.2 mA/cm^2 and 0.083 for Passive 2 flux (Theoretical). Thus, there are two mechanisms for flux enhancement relative to passive flux on "fresh" HMS: (a) the effect of the voltage drop in increasing mass transfer over the passive diffusion level, the effect of electroosmotic flow dominating this contribution in the systems studied here, and (b) the effect of prior current flow in increasing the "intrinsic permeability." Both effects appear to be significant (Fig. 4).

Based on the theoretical results given in detail elsewhere (1) and outlined in this report, theoretical values for solution flux, J_{vs}, in μl/hr cm^2, were calculated using input data summarized in Table I. The comparison of theoretical and experimental fluxes (0.1 *M* NaCl) is summarized in Fig. 6, where the experimental values are given in dark shading, and the theoretical values are given in lighter shading. In these calculations, anodic flux occurs mostly through the large (27-Å) negative pores, cathodic flux is largely via the neutral (13.5-Å) and positive (6.75-Å) pores, and passive flux

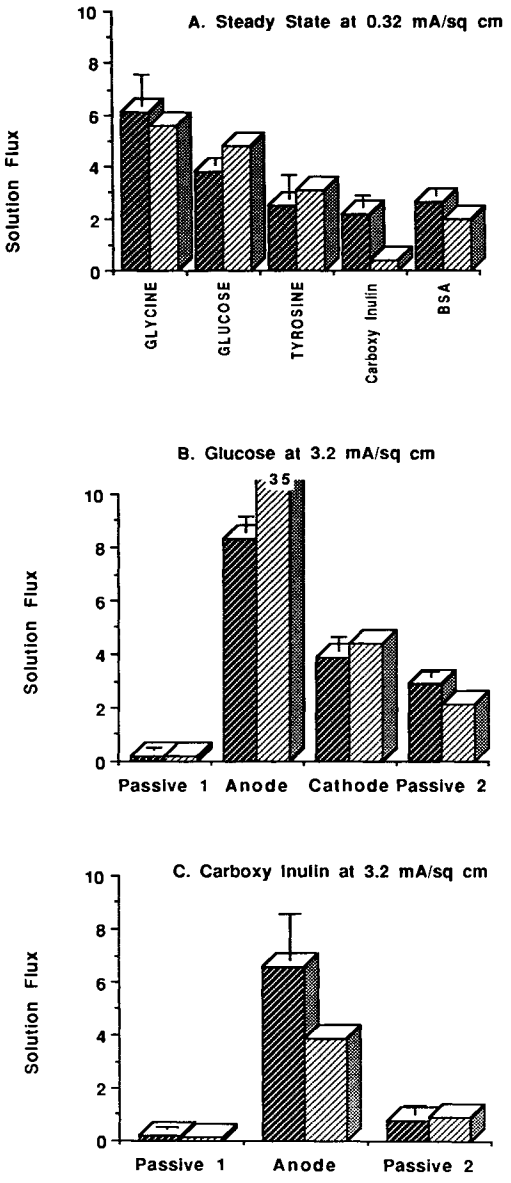

Fig. 6. Comparison of theory and experiment. Solution flux is J_{vs} in μl/hr cm^2 at 37°C in 0.1 *M* NaCl. Experimental values are in dark shading, and theoretical values are in light shading. The error bars are standard errors. All theoretical values are calculated for steady state assuming all reflection coefficients are zero. Experimental values given in A are steady-state values (16-hr time), but B and C refer to a time of 1.5 hr and are not necessarily steady state.

has significant contributions from all pore types. It is significant to note that with only two exceptions, the calculated fluxes are essentially in quantitative agreement with the experimental values. Agreement is essentially within experimental error for all passive flux comparisons, and the lack of quantitative agreement is restricted to iontophoretic flux. The calculated flux for carboxy inulin at 0.32 mA/cm^2 appears significantly lower than the measured flux, and the calculated flux for glucose at 3.2 mA/cm^2 is about a factor of 4 higher than observed. Calculated glucose fluxes for 0.05 *M* NaCl and 0.5 *M* NaCl are also about a factor of 4 higher than observed. Thus, the trend with NaCl concentration is correctly predicted, but the absolute value of the glucose flux is not quantitative. Note that the calculated and observed values are in good agreement at 0.32 mA/cm^2. While it is likely that the experiments used to determine glucose flux at 3.2 mA/cm^2 were not at steady state, which qualitatively would cause the observed deviation from theory, it should be noted that the agreement between theoretical and experimental cathodic fluxes is excellent. Since we cannot argue that the approach to steady state should be faster for cathodic delivery, it would appear that either the anodic or the cathodic fluxes for glucose deviate quantitatively from theory at high current density.

Agreement between theory and experiment for cathodic delivery of carboxy inulin (not shown) is also not quantitative. The theoretical flux is much higher (92 μl/hr cm^2) than the measured flux (1.7 ± 0.3 μl/hr cm^2). In this case, all flux originates from positive pores (63%) or neutral pores (37%). Since the Stokes radius for carboxy inulin is about twice the pore radius of the positive pores, one would expect a high reflection coefficient and little or no transport contribution from the positive pores. However, even if the flux from positive pores is assumed to be zero, the theoretical flux (through neutral pores) is about a factor of 20 higher than the experimental flux. It *appears* that the reflection coefficient of inulin in the neutral pores (slightly larger than the Stokes radius) is near unity. Yet the good agreement between theory and experiment for anodic BSA flux suggests minimal reflection of BSA from negative pores, which are slightly smaller than the Stokes radius (35 Å). The origin of the inconsistency likely resides in the pore distribution model assumed by the theory (1). The relationship between pore sizes for the three different pores was arbitrarily assumed to be at the ratio 0.5:1.2 for the three pore types positive:neutral:negative.

The concept that not all pores have the same charge was introduced to reconcile transference number, electrical resistance, and electroosmotic flow data (1). Heterogeneity in pore charge is also required to explain some of the flux data obtained in the present study. For example, although HMS has a *net* negative charge (2), a membrane consisting entirely of negative pores would produce zero cathodic flux of a neutral species due to unfavorable electroosmotic flow, whereas the observed cathodic flux of glucose is 3.9 ± 0.5 μl/hr cm^2. A homogeneous pore model constrained to be consistent with volume flow data (1) would also predict zero anodic flux for carboxy inulin at pH 8.5, contrary to observation. Therefore, the concept of a heterogeneous pore system with the larger pores having, on the average, a higher concentration of negative charge seems valid. However, quantitative details of the pore distribution, particularly those involving positive and neutral pores, are probably not a good approximation to the more complex actual pore system. Since no attempt was made to obtain a "best fit" of pore system radii and charge to all the available data, such deficiencies in the model are understandable.

REFERENCES

1. M. J. Pikal. *Pharm. Res.* 7:118–126 (1990).
2. M. J. Pikal and S. Shah. *Pharm. Res.* 7:213–221 (1990).
3. R. Burnette and D. Marrero. *J. Pharm. Sci.* 75:738–743 (1986).
4. R. Burnette and B. Ongpipattanakul. *J. Pharm. Sci.* 76:765–773 (1987).
5. L. Gangarosa, N. Park, C. Wiggins, and J. Hill. *J. Pharmacol. Exp. Ther.* 212:377–381 (1980).
6. R. R. Burnette and T. M. Bagniefski. *J. Pharm. Sci.* 77:492–497 (1988).
7. C. R. Cantor and P. R. Schimmel. *Biophysical Chemistry,* Part I, W. H. Freeman, San Francisco, 1980.
8. P. L. Altman. In D. S. Dittmer (ed.), *Biological Handbooks: Blood and Other Body Fluids,* Federation of American Society for Experimental Biology, Washington, D.C., 1961 p. 47.
9. N. Lakshminarayanaiah. *Chem. Rev.* 65:491–565 (1965).
10. Y. C. Chang and A. S. Myerson. *AIChE J.* 32:1567–1569 (1986).
11. J. K. Gladden and M. Dole. *J. Am. Chem. Soc.* 75:3900–3904 (1953).
12. J. Duclaux, W. Zasepa, and A. Dobry-Duclaux. *J. Chim. Phys.* 63:669–674 (1966).
13. R. C. Lanman, J. A. Burton, and L. S. Schanker. *Life Sci.* 10 (part 2):803–811 (1971).
14. K. H. Keller, E. R. Canales, and S. I. Yum. *J. Phys. Chem.* 75:379–387 (1971).
15. G. Manning. *Annu. Rev. Phys. Chem.* 117–140 (1972).
16. J. C. Keister and G. B. Kasting. *J. Membrane Sci.* 29:155–167 (1986).
17. H. Rein. *Z. Biol.* 81:125–140 (1924).